

## Supplementary Information

### Triggering Nanoparticle Surface Ligand Rearrangement via External Stimuli: Light-based Actuation of Biointerfaces

Zhenghua Tang,<sup>1,†,‡</sup> Chang-Keun Lim,<sup>2,3,‡</sup> J. Pablo Palafox-Hernandez,<sup>4,‡</sup> Kurt L.M. Drew,<sup>4</sup> Yue Li,<sup>3,5</sup> Mark T. Swihart,<sup>3,5</sup> Paras N. Prasad,<sup>2,3,6,\*</sup> Tiffany R. Walsh,<sup>4,\*</sup> and Marc R. Knecht<sup>1,\*</sup>

<sup>1</sup>University of Miami, Department of Chemistry, Coral Gables, Florida 33146, United States,

<sup>2</sup>Department of Chemistry, <sup>3</sup>Institute for Laser Photonics and Biophotonics, University at Buffalo (SUNY), Buffalo, New York 14260, United States, <sup>4</sup>Institute for Frontier Materials, Deakin University, Geelong, Victoria 3216, Australia, <sup>5</sup>Department of Chemical and Biological Engineering, University at Buffalo (SUNY), Buffalo, New York 14260, United States, and

<sup>6</sup>Department of Chemistry, Korea University, Seoul 151-747, Korea.

\*To whom correspondence should be addressed:

PNP: [pnprasad@buffalo.edu](mailto:pnprasad@buffalo.edu); TRW: [tiffany.walsh@deakin.edu.au](mailto:tiffany.walsh@deakin.edu.au); MRK: [knecht@miami.edu](mailto:knecht@miami.edu)

## Additional Methodology

**Force-field details:** The MAM unit (see Scheme 1 in the main text) was built using the software package Avogadro<sup>1</sup>. Most bond lengths, bond angles and dihedral angles in the MAM unit were adequately captured using existing terms in the CHARMM36 force-field<sup>2</sup>. The chief exception to this was the dihedral associated with the central N=N bond. For this dihedral angle, parameters were set to ensure the MAM remained in either the *trans* (180° dihedral angle) or *cis* (0° dihedral angle) state. The optimal dihedral angle parameters for the aryl rings adjacent to the central N=N bond were taken from our extensive electronic structure theory calculations based on similar systems<sup>3</sup>. For the non-bonded Lennard-Jones interactions, existing parameters from the CHARMM36 force-field were used. Partial charges for the MAM unit were assigned based on estimates obtained using ParamChem<sup>4</sup> online server, adjusted to ensure harmonization with the charges on the AuBP1-C and C-AuBP1 peptides. The GoIP-CHARMM force-field contains bespoke pair interactions for certain CHARMM atom types, some of which are present in the MAM unit; the central nitrogen atoms in the MAM unit were also assigned bespoke interactions with the Au slab surface sites.

### Replica Exchange with Solute Tempering Molecular Dynamics Simulations:

REST Details: Our implementation of REST uses the replica exchange and free energy perturbation theory codes within Gromacs 4.5.5<sup>5</sup>. Details of the Terakawa<sup>6</sup> implementation of REST have been given by us elsewhere<sup>7,8</sup>. In our REST simulations, we spanned an ‘effective temperature’ window of 300-430K with 16 replicas. The initial configurations for each replica cover a range of secondary structures, including  $\alpha$ -helix,  $\beta$ -turn, polyproline II and random coil conformations for the peptide component of the molecule, and either the *trans* or the *cis* conformation for the MAM component of the molecule. The adsorbate structure for each replica was initially placed so that at least one peptide atom was within  $\sim 3\text{\AA}$  distance from the top surface of the Au slab. The 16 values of lambda used to scale our force-field were:

$\lambda_j = 0.0000, 0.057, 0.114, 0.177, 0.240, 0.310, 0.382, 0.458, 0.528, 0.597, 0.692, 0.750, 0.803, 0.855, 0.930, 1.0000$ .

Following Wright *et al.*<sup>8</sup>, only the bond-stretching, dihedral, and non-bonded terms of the intra-peptide potential were scaled for each replica. Before initiating the REST run, initial configurations were equilibrated at their target potential for 0.5 ns, with no exchange moves attempted in this period. The interval between exchange attempts set to 1000 MD steps (every 1 ps). All production REST simulations were run for a total of  $25 \times 10^6$  MD steps (25 ns).

**Table S1:** Residue-surface contact data (percentage). Anchor residues (with a contact percentage  $\geq 60\%$ ) are highlighted in green. \*Previous work (*Chem. Mat.* **2014**, 26, 4960–4969).

<b>Residue</b>	<b>MAM-CAuBP1</b>	<b>AuBP1C-MAM</b>	<b>AuBP1 parent*</b>
<b>MAM</b>	<b>96</b>	---	---
<b>C</b>	56	---	---
<b>W</b>	<b>76</b>	<b>75</b>	<b>84</b>
<b>A</b>	28	4	48
<b>G</b>	38	3	<b>66</b>
<b>A</b>	34	16	58
<b>K</b>	42	37	22
<b>R</b>	58	<b>81</b>	<b>92</b>
<b>L</b>	15	17	46
<b>V</b>	20	43	39
<b>L</b>	36	17	49
<b>R</b>	35	<b>66</b>	<b>77</b>
<b>R</b>	<b>67</b>	40	<b>85</b>
<b>E</b>	53	28	50
<b>C</b>	---	<b>90</b>	---
<b>MAM</b>	---	<b>97</b>	---

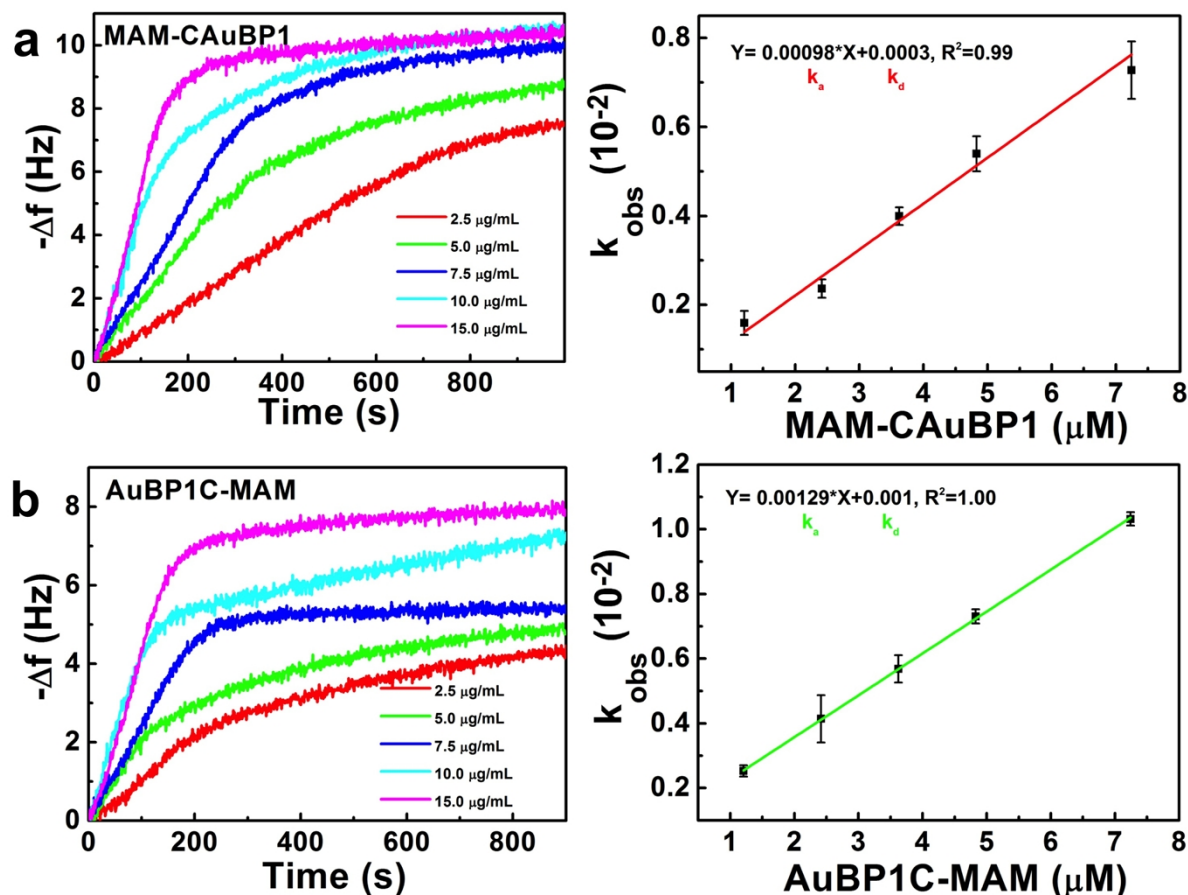


**Figure S1.** QCM analysis of the binding of (a) MAM-CAuBP1 and (b) AuBP1C-MAM peptides to Au with the MAM unit in the *trans* conformation. The left image displays the change in resonating frequency of the Au sensor surface, which was fit using a Langmuir isotherm to determine  $k_{\text{obs}}$  values. The right panels plot the determine  $k_{\text{obs}}$  values as a function of peptide solution concentration, from which the  $k_a$  and  $k_d$  values can be ascertained as the slope and  $y$ -intercept, respectively. From this, the  $K_{\text{eq}}$  and  $\Delta G$  of binding can be calculated.

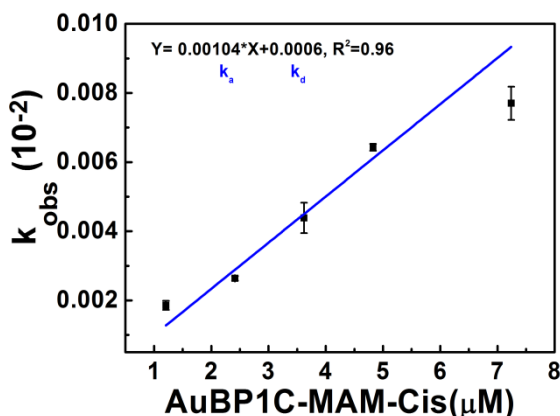
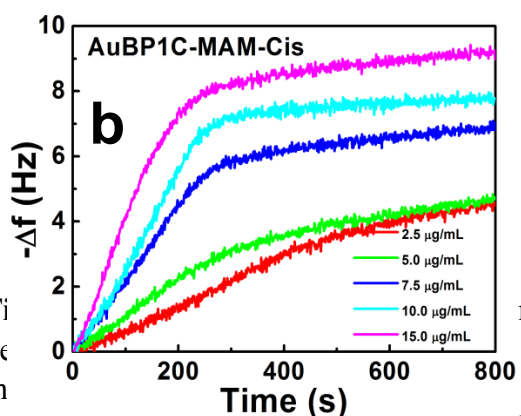
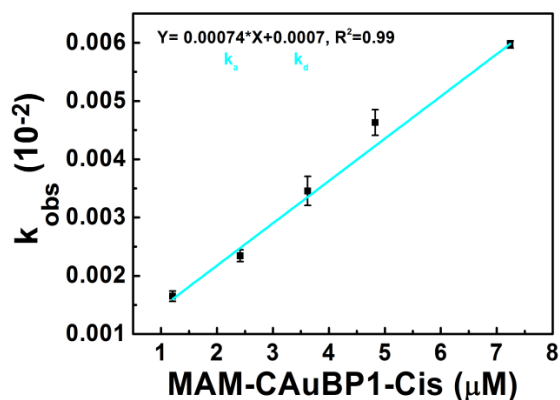
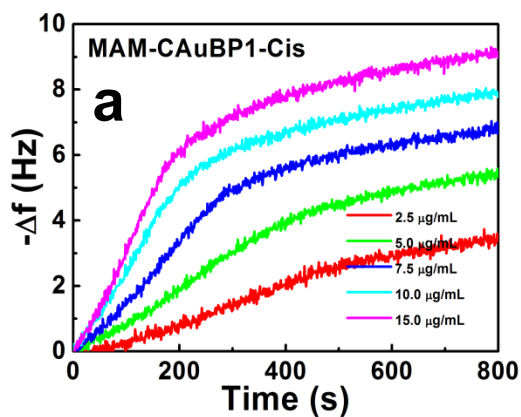
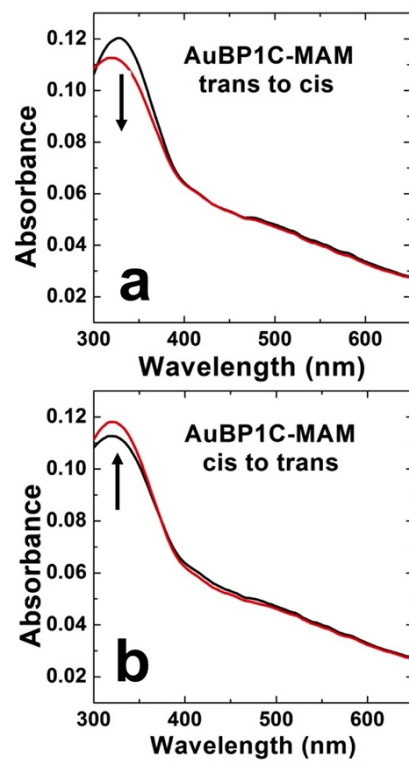
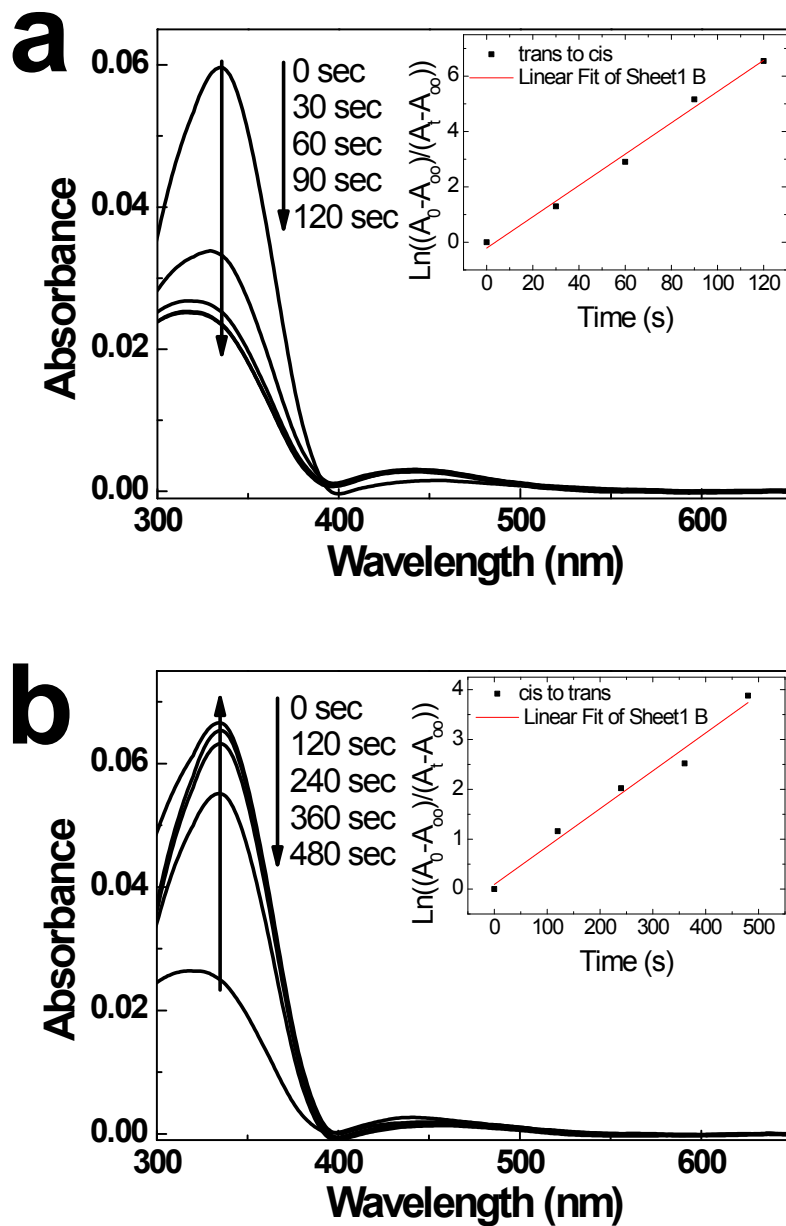


Figure 1. (a) Sensorgrams of MAM-CAuBP1-Cis. (b) Plot of  $k_{obs}$  values as a function of peptide solution concentration, from which the  $k_a$  and  $k_d$  values can be ascertained as the slope and y-intercept, respectively. From this, the  $K_{eq}$  and  $\Delta G$  of binding can be calculated.



**Figure S3.** Photoswitching analysis of the MAM-CAuBP1 peptide bound to Au NPs for the (a) *trans* to *cis* and (b) *cis* to *trans* transitions.



**Figure S4.** Time-dependent photoswitching analysis of the (a) *trans* to *cis* and (b) *cis* to *trans* isomerization of free MAM in DMF. Insets show plots of first-order rate law.

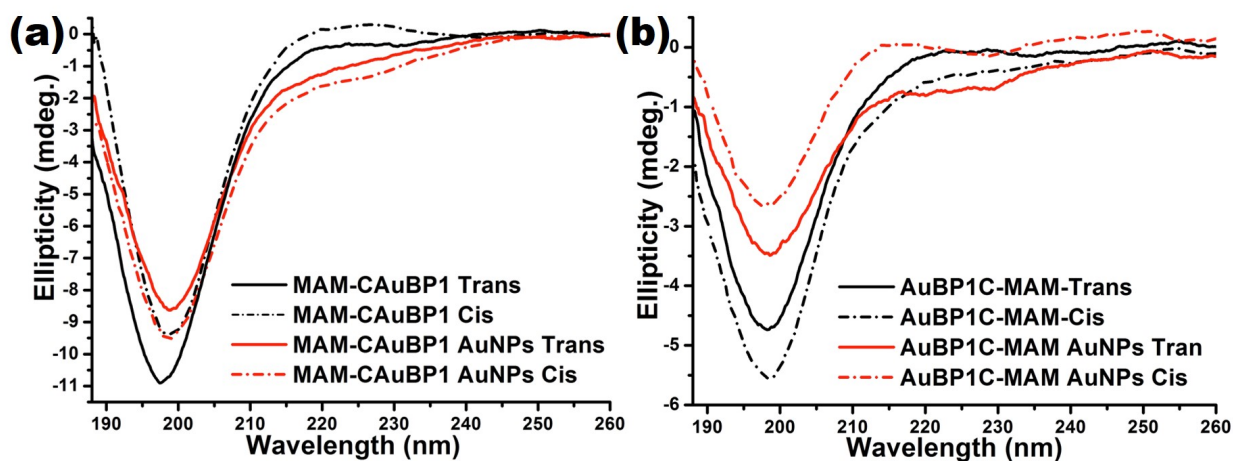


**Figure S5.** CD spectra of unbound peptides (black curves) and Au nanoparticle-bound peptides (red curves) in *trans* (solid curves) and *cis* (dashed curves) conformations of the (a) MAM-CAuBP1 and (b) AuBP1C-MAM. Note that the change in ellipticity upon switching is in opposite directions for the bound and unbound peptides.

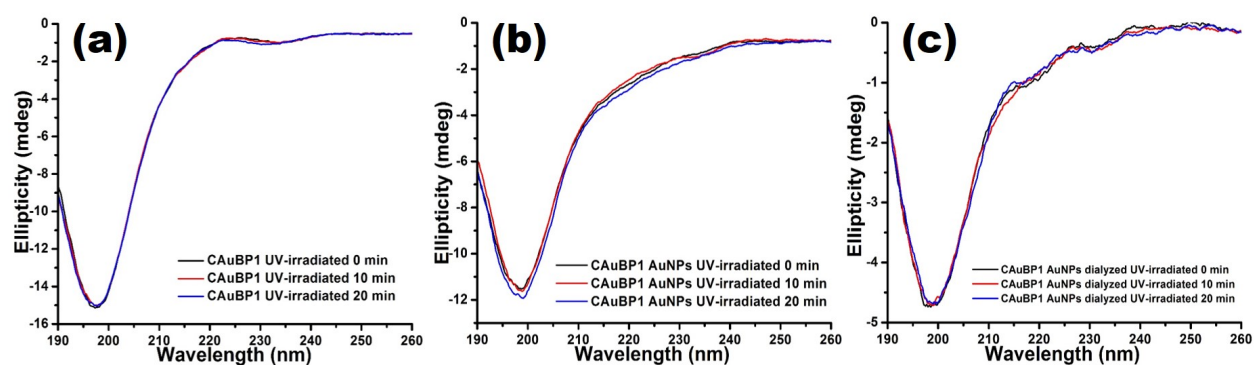


**Figure S6.** CD spectra of the CAuBP1 peptide, without MAM incorporation, before and after irradiation with 365nm UV light for different time intervals. Part (a) is the unbound, free peptide, while parts (b) and (c) are for the CAuBP1-capped AuNPs before and after dialysis, respectively, which removes unbound peptide, but may also reduce the peptide coverage on the AuNP surface as the surface equilibrates with the solution concentration. Note that no change in the CD spectra are observed as no peptide structural changes are evident in the absence of the MAM based upon light irradiation.

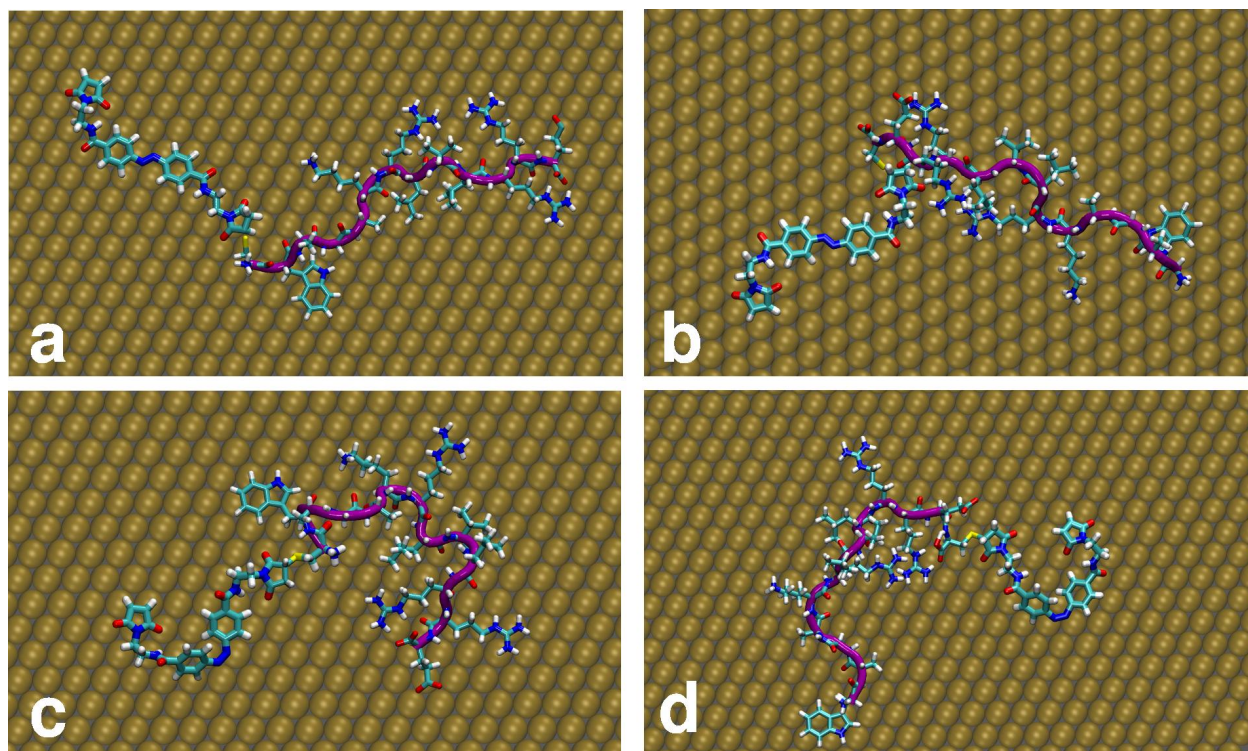


**Figure S7.** Snapshots of the most likely structures of the molecules adsorbed at the aqueous Au(111) interface, predicted from REST simulations, shown in plan view. In each case, the peptide backbone is indicated in purple. (a) *trans* AuBP1C-MAM, (b) *trans* MAM-CAuBP1, (c) *cis* AuBP1C-MAM, and (d) *cis* MAM-CAuBP1.

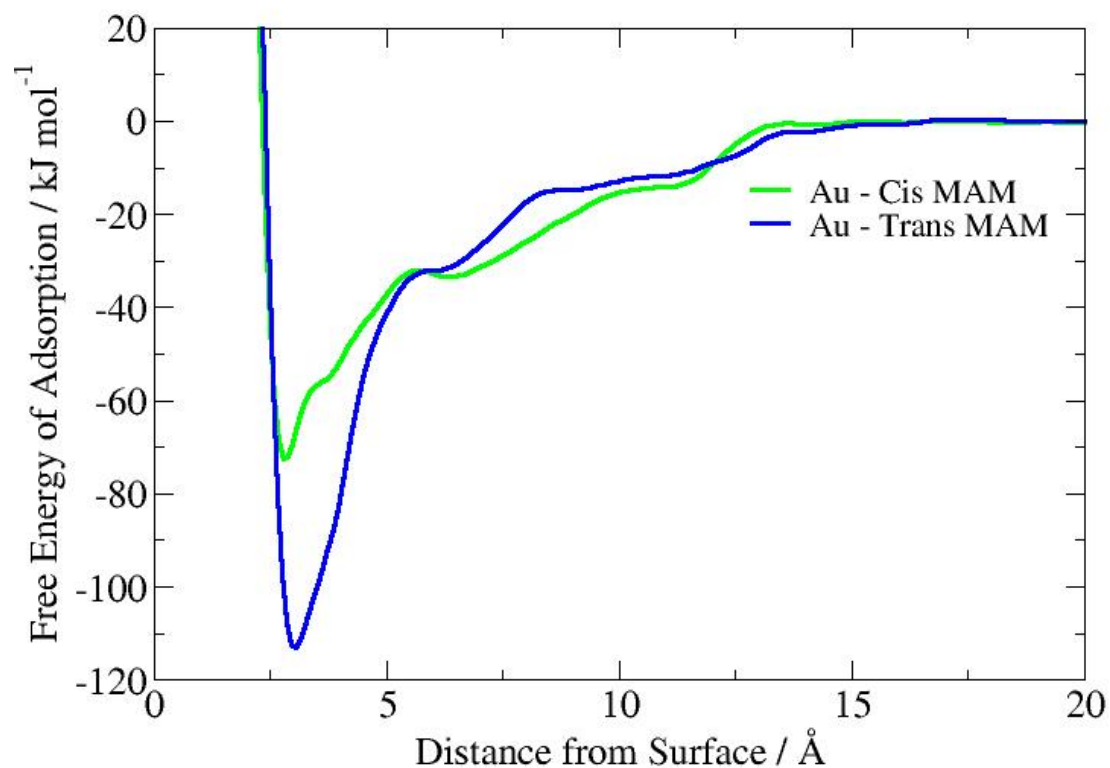


**Figure S8.** Change in free energy of adsorption for the free MAM unit in both the *trans* and *cis* states, at the aqueous Au(111) interface, calculated using well-tempered metadynamics simulations.

## References

- (1) Hanwell, M. D.; Curtis, D. E.; Lonie, D. C.; Vandermeersch, T.; Zurek, E.; Hutchison, G. R. *J. Cheminf.*, **2012**, *4*:17.
- (2) Klauda, J. B.; Venable, R. M.; Freites, J. A.; O'Connor, J. W.; Tobias, D. J.; Mondragon-Ramirez, C.; Pastor, R. W. *J. Phys. Chem. B*, **2011**, *114*, 7830-7843.
- (3) Hough A. J.; Prokes I.; Tucker J. H. R.; Shipman M.; Walsh T. R. *Chem. Commun.*, **2013**, 49, 6683-6685.
- (4) Vanommeslaeghe K., MacKerell Jr. A. D. *J. Chem. Inf. Model.* 2012, *52*, 3144-3154; Vanommeslaeghe K., MacKerell Jr. A. D. *J. Chem. Inf. Model.* 2012, *52*, 3155-3168; <https://cgenff.paramchem.org>
- (5) Hess, B.; Kutzner, C.; van der Spoel, D.; Lindahl, E. *J. Chem. Theor. Comp.* **2008**, *4*, 435–447.
- (6) Terakawa, T.; Kameda, T.; Takada, S., *J. Comput. Chem.* **2011**, *32*, 1228-1234.
- (7) Palafox-Hernandez J. P.; Tang, Z.; Hughes, Z. E., Li, Y.; Swihart, M. T.; Prasad, P. N. Walsh T. R.; Knecht M. R. *Chem. Mat.* **2014**, *26*, 4960–4969.
- (8) Wright, L. B.; Walsh, T. R., *Phys. Chem. Chem. Phys.* **2013**, *15*, 4715-4726.